

Vimentin intermediate filament and plectin provide a scaffold for invadopodia,
facilitating cancer cell invasion and extravasation for metastasis

(ビメンチン中間径フィラメントとプレクチンによる浸潤突起の足場形成は癌転移のための
浸潤および血管外脱出過程を促進する)

申請者	弘前大学大学院医学研究科
	腫瘍制御科学領域 泌尿器腫瘍学教育研究分野
氏 名	米山 美穂子
指導教授	大山 力

ABSTRACT

To investigate the molecular mechanisms of cancer metastasis, we have isolated a high-metastatic bladder cancer cell subpopulation from a low-metastatic cell line by using an *in vivo* selection system. Cells in the subpopulation showed a high ability to form invadopodia, the filamentous actin (F-actin)-based membrane protrusions that play an essential role in cancer cell invasion. Analysis of the gene expression profile revealed that the expression of an intermediate filament (IF) protein, vimentin and a cytoskeletal linker protein, plectin was up-regulated in the high-metastatic subpopulation compared with the low metastatic cell line. Here we report a novel role of vimentin IF and plectin in metastasis. In invasive bladder cancer cells, the vimentin IF-plectin-invadopodia F-actin link was formed. Disruption of this link severely impaired invadopodia formation, reducing the capacities of extracellular matrix degradation, transendothelial migration and metastasis. In addition, the vimentin assembly into the filaments was required for invadopodia formation. Our results suggest that plectin anchoring invadopodia to vimentin IF scaffolds and stabilizes invadopodia, which is a critical molecular process for cancer cell invasion and extravasation for metastasis.

Keywords: cancer cell extravasation / invadopodium / invadosome / invasion / plectin / vimentin

Introduction

The major cause of mortality in patients with cancer is metastasis. Among the multiple processes involved in metastasis, cancer cell invasion is considered a key process. For cancer cell invasion process, highly invasive cancer cells form invadopodia, the filamentous actin (F-actin)-based membrane protrusions to remodel extracellular matrix (ECM) and invade surrounding tissues. Invadopodia are specialized to degrade ECM (Even-Ram and Yamada, 2005) and enriched with a variety of proteins including actin and actin regulatory proteins, matrix-degrading enzymes, signalling molecules and membrane remodelling proteins (Ayala et al., 2008; Buccione et al., 2009). Although invadopodia are considered to play important roles in the steps of the metastatic cascade, the details of the invadopodia formation have not been fully understood yet.

Invasive cancer cells metastasize haematogenously and lymphogenously. Haematogenous metastasis includes two invasion processes. Invasive cancer cells escape from the primary site into nearby blood vessels (intravasation). The disseminating cancer cells exit the vessels to invade across endothelia into the tissue of a secondary organ (extravasation) (Gupta and Massague, 2006). In the case of patients with invasive bladder cancer, the most common site of haematogenous metastasis is lung (Smith et al., 2009). In the extravasation process, the circulating bladder cancer cells eventually exit the microvessels in lung via migration across

endothelia. Cells invade lung tissues and proliferate to form metastases. To elucidate molecular mechanisms of bladder cancer cell extravasation and colonization, we employed an *in vivo* selection system that mimics a late stage of haematogenous metastasis of bladder cancer (including dissemination, extravasation, invasion and colonization) on a low-metastatic bladder cancer cell line, KK-47. We successfully isolated a high-metastatic subpopulation, KK-47HM4 which showed a high capacity of extravasation (Sugiyama et al., 2013). KK-47HM4 cells exhibited significantly higher capacities of *in vitro* migration through both extracellular matrix (ECM) and endothelia than KK-47 cells (Sugiyama et al., 2013), suggesting that KK-47HM4 cells possess a high capacity to extravasate from the lung microvessels and invade the lung tissues. These results led us to postulate that the KK-47HM4 subpopulation can be a helpful tool for investigation into the molecular mechanisms of cancer cell extravasation and invasion. We thus performed cDNA microarray analysis to make a comparison of the gene expression between KK-47 and KK-47HM4 and identified 67 genes whose expression was up- or down-regulated in KK-47HM4 cells (Sugiyama et al., 2013).

We have recently demonstrated that the extravasation of bladder cancer cells requires the formation of invadopodia (Tokui et al., 2014). In this study, we investigated the process of invadopodia formation which is required for cancer cell extravasation and invasion for metastasis by using the information from the cDNA microarray analysis.

Materials and methods

Cells, antibodies and reagents

Six established human bladder cancer cell lines were used. KK-47 (Kubota et al., 1996), YTS-1 (Hisazumi et al., 1981) and BOY (Kayajima et al., 1989) were the generous gifts of Drs. T. Matsuo (Tohoku University, Japan), H. Kakizaki (Yamagata University, Japan) and M. Nakajima (Kagoshima University, Japan), respectively. RT-4, 5637, BOY and T24 were purchased from American Type Culture Collection (ATCC). Primary culture of bladder cancer cells was prepared as described before from bladder tumours which were surgically removed from several genetically independent patients at Department of Urology, Hirosaki University Graduate School of Medicine (Hirosaki, Japan) (Sutoh et al., 2010). Tumour stages were determined according to the American Joint Committee for Cancer Staging. Written consents were obtained from all the patients. The institutional review board of Hirosaki University Graduate School of Medicine approved this study. All the bladder cancer cells were maintained in RPMI 1640 medium (Sigma-Aldrich) supplemented with 10% fetal bovine serum (FBS) (PAA Laboratories). Primary human microvascular endothelial cells from lung (HMVEC-L) were purchased from Lonza and maintained in EGM-2MV medium. All cells were grown at 37°C and 5% CO₂ in a humidified incubator. All the biochemical reagents were purchased

from Sigma-Aldrich, unless otherwise noted. The monoclonal antibodies to plectin (10F6, eBioscience and E398P, abcam), vimentin (V9, Sigma-Aldrich and EPR3776, abcam), cortactin (EP1922Y, EPITOMICS), uroplakin III (SP73, Spring Bioscience) and glyceraldehyde-3-phosphate dehydrogenase (GAPDH) (3H12, MBL) and a polyclonal antibody to actin (Sigma-Aldrich) were used in this study.

Immunoprecipitation and western blotting

For immunoprecipitation of plectin or vimentin from cells, cytoskeletal fraction was enriched by using ProteoExtract Cytoskeleton Enrichment and Isolation Kit (Millipore). The resultant cytoskeletal fraction was incubated with anti-plectin (10F6, 2 µg/ml) or anti-vimentin monoclonal antibody (V9, 1 µg/ml), and then incubated with anti-mouse IgG agarose (Sigma-Aldrich). The agarose resin was washed and the immune complex was eluted with 1x Laemli's SDS-PAGE sample buffer. The sample was subjected to SDS-PAGE gel (Invitrogen, USA), and transferred onto PVDF membrane. Western blotting analysis was performed using the specific antibodies and a horseradish peroxidase-conjugated secondary antibody. Signals were visualized using the ECL+PLUS detection system (GE Healthcare, USA) and ATTO Chemilluminescence Imaging System EZ-Capture II (ATTO, Japan).

Visualization of invadopodia and immunofluorescence Microscopy

Cells were fixed in 4% paraformaldehyde and permeabilized with PBS containing 0.1% saponin and 1% bovine serum albumin (BSA). Cells were stained with Alexa Fluor 568-labelled phalloidin (Invitrogen) and antibodies. Cell staining was examined under a fluorescence microscope (Olympus IX-71) and LSM 710 Laser Scanning confocal microscope (Carl Zeiss). Invadopodia are visualized as puncta where F-actin and cortactin (an invadopodium marker) co-localize (Oser et al., 2009).

Matrigel degradation assay

Laminin (BD Biosciences) was labelled with Alexa Fluor 488 with Protein Labelling kit (Invitrogen). Membranes of the transwell insert were coated with 80 µl with a 1:1 mix of 9.7 mg/ml Matrigel (BD Biosciences) with 0.5 mg/ml of labelled laminin for 1 h at 4°C and then 45 µl was removed and the inserts were incubated at 37°C for overnight for polymerization of Matrigel. Cells (5×10^4) were added to the insert. After 2 h incubation at 37°C, migrated cells were fixed and stained with Alex Fluor 568-labelled phalloidin. Membranes were cut out of inserts and cells were imaged with an LSM 710 laser scanning confocal microscope (Carl Zeiss).

Stable transfectants

YTS-1 cell lines with reduced expression of plectin (plectin knockdown cells, PIKD) and vimentin (vimentin knockdown cells, ViKD) were generated by shRNA technology (Seals et al., 2005; Tsuboi et al., 2011). Synthesized primers designed to express a short hairpin RNA (shRNA) for the direct targeting and knockdown of plectin and vimentin mRNA sequences. The shRNA expression plasmids were constructed using pBAsi-hU6Neo DNA (Takara Bio. Inc., Japan). We used the following siRNA sequences (siPlectin-1, siPlectin-2 and siVimentin). The siRNA sequences were : 5'-cgcgactcatcttgcgtg-3' (siPlectin-1); 5'-catttgaagagacacagatcg-3' (siPlectin-2); 5'-gtacgtcagcaatatgaaa-3' (siVimentin). A non-targeting siRNA sequence (Accell siRNA control, Thermo Scientific) was used to prepare the control cells expressing non-targeting shRNA. To rescue the expression of plectin protein in plectin knockdown cells, we took advantage of the fact that only 15 out of 19 and 16 out of 21 base pairs encompassing siPlectin-1 and siPlectin-2, respectively are conserved in the mouse plectin cDNA. PIKD-1 cells were transfected with a mouse plectin expression plasmid (pCMV-mouse plectin). The results obtained by one representative rescue clone (designated PIKD-1+mPl) were shown here.

Matrigel invasion and transendothelial migration assays

Matrigel invasion assay was performed as previously described (Sutoh et al., 2010). For transendothelial migration assay, HMVEC-L cells (1×10^5) were placed onto collagen I-coated upper chamber of the transwell insert and cultured over 2 days to form a monolayer. Bladder cancer cells (5×10^4) were labelled with Vybrant CFDA SE cell Tracker Kit (Invitrogen) and then placed into the upper chamber. After incubation at 37°C for 24 h, migrated cells were fixed and counted (Sugiyama et al., 2013 ; Tokui et al., 2014).

Gelatin zymography

Gelatin zymography was performed using 10% pre-cast SDS-polyacrylamide gel (Cosmo Bio Co., Ltd., Tokyo, Japan) in the presence of 0.1% gelatin (Invitrogen), as previously described (Sutoh et al., 2010). Briefly, conditioned media from bladder cancer cells were collected and subjected to SDS-PAGE. Gels were washed in 2.5% Triton X-100 for 30 min at room temperature, incubated at 37°C overnight in substrate buffer containing CaCl_2 and then stained with 0.5% Coomassie Brilliant Blue R-250 in 50% methanol and 10% acetic acid for 1h. MMP marker (Cosmo Bio Co., Ltd.) was used as a matrix metalloproteinase marker.

Lung metastasis assay in nude mice

Lung metastasis assay was performed as previously described (Tokui et al., 2014). Briefly, bladder cancer cells (2×10^6) were injected into the tail vein of nude mice (BALB/cAJcl-nu/nu) (Clea Japan, Japan). After three weeks, lungs were harvested and fixed with formalin. The metastasized tumor area was determined by hematoxylin and eosin (HE) staining combined with anti-uropelakin III (human bladder cancer marker) staining (Amin, 2009). The committee for animal experiments of Oyokyo Kidney Research Institute approved these experiments.

Statistical analysis

We used the statistical program SPSS 12.0 (SPSS). Statistically significant differences were determined using the Student's *t*-test, unless otherwise noted. For the comparison of lung metastasis, Mann-Whitney *u*-test was used to assess statistical significance between two groups. Differences were considered significant, if $P < 0.05$.

Results

Increased expression of vimentin and plectin in invasive cancer cells

In order for invasive cancer cells to degrade ECM and invade surrounding tissues, the cancer cells form invadopodia (Buccione et al., 2009; Linder, 2009; Murphy and Courtneidge, 2011). We previously reported that the invasive bladder cancer cells formed invadopodia but that the non-invasive bladder cancer cells barely formed invadopodia (Sutoh et al., 2010; Yamamoto et al., 2011). We examined the invadopodia formation in KK-47HM4, since we previously showed that KK-47HM4 exhibited a higher capacity of extravasation than KK-47 (Sugiyama et al., 2013) and extravasation of invasive bladder cancer cells required invadopodia formation (Tokui et al., 2014). Few invadopodia were observed in a KK-47 cell (Figs. 1A and 1C). In contrast, numbers of F-actin puncta where cortactin co-localizes were observed in KK-47HM4 cells (Figs. 1B and 1C). We showed that KK-47HM4 cells secrete matrix-metalloproteinases much more than KK-47 cells (Supplementary Fig. 2, lanes 2 and 3) and that these F-actin-based structures have an ability to degrade Matrigel matrix (Fig. 1D). In addition, we previously showed that KK-47HM4 cells exhibited a higher Matrigel invasion activity than KK-47 cells (Sugiyama et al., 2013). These results taken together indicate that KK-47HM4 cells form the

functional invadopodia, suggesting that the higher extravasation capacity of KK-47HM4 is due to the higher ability to form invadopodia.

We then asked what factors are involved in invadopodia formation in KK-47HM4 cells. To address this question, we performed cDNA microarray analysis and identified 67 genes whose expression was up- or down-regulated in KK-47HM4 cells compared with KK-47 cells (Sugiyama et al., 2013). These could include some genes which are potentially involved in invadopodia formation. It has been reported that regulation of the actin cytoskeleton is essential for invadopodia formation leading to invasion and metastasis of cancer cells by promoting a variety of cellular processes such as changes in morphology, motility and adhesion (Clark et al., 2000; Jaffe and Hall, 2002). We thus chose vimentin and plectin which meet this criterion from the up-regulated genes in KK-47HM4 cells.

Vimentin is an intermediate filament (IF) protein that regulates cell migration in many cell types (Ivaska et al., 2007). Vimentin molecule is constituted by a globular non- α -helical N-terminal head, a central coiled-coil domain and a C-terminal tail domain (Fig. 1E). The assembly of vimentin into long 10-12 nm calibre polymers is controlled by its head domain (Favre et al., 2011). Vimentin expression is induced in numbers of invasive cancers and the high expression of vimentin in cancer well correlates with increased invasion, metastasis and poor prognosis (Satelli and Li, 2011).

Plectin is a widely expressed cytoskeletal linker protein of > 500 kDa that has important functions in mediating interactions between different cytoskeletal networks (Wiche and Winter, 2011). Plectin has a multi-domain structure with three main sections: a central rod domain flanked by N- and C-terminal regions (Fig. 1E). Plectin possesses binding sites for all types of IFs including vimentin, cytokeratin and desmin in its C-terminal region. Its N-terminal region contains a functional F-actin binding domain (ABD) (Fig. 1E). Although the roles of plectin in epithelial cells and skeletal muscle are quite understood (Wiche and Winter, 2011; Winter and Wiche, 2013), little is known about its role in invasive cancer cells.

The expression levels of vimentin and plectin were increased in KK-47HM4 cells compared with KK-47 cells (Fig. 1F, lanes 1-4; Fig. 3, lanes 1-4), but no significant changes in the expression levels of actin and glyceraldehyde-3-phosphate dehydrogenase (GAPDH) (Fig. 1F, lanes 5-8; Fig. 3, lanes 5-8). In addition, western blots showed the increased levels of vimentin and plectin in the invasive bladder cancer cell lines, T24, BOY and YTS-1, compared with the non-invasive bladder cancer cell lines, RT4 and 5637 (Fig. 1F, lanes 9-18). To validate these results by physiologically relevant materials, we prepared primary culture cells from the bladder cancer specimens of three patients, Patient 1, 2 and 3. (Patient profiles described in Fig. 4A). Western blots showed that the expression levels of vimentin and plectin were increased in cultured primary cells from Patient 2 and 3 with invasive bladder cancer, compared with Patient 1 with non-invasive bladder cancer (Fig. 1F, lanes 29-34). In fact, although few invadopodia

were formed in the bladder cancer primary culture cells from Patient 1, numbers of invadopodia with a high ECM degradation activity were formed in the cells from Patient 3 (Fig. 4B, C) as well as Patient 2 (data not shown). These results taken together indicate that the increased expression of vimentin and plectin is associated with the high ability to form invadopodia and the invasive capacity. Based on these results (Fig. 1) and our previous study (Sugiyama et al., 2013), we hypothesized that the increased expression of vimentin and plectin contributes to invadopodia formation, resulting in higher invasive capacity. To test this hypothesis, we focused on investigating the role of vimentin IF and plectin in invadopodia formation.

Formation of the vimentin IF-plectin-invadopodia F-actin link in invasive cancer cells

To examine if plectin functions as a cytolinker in invasive cancer cells, we first prepared cytoskeletal fractions from invasive bladder cancer cells, YTS-1 and Patient 3. Monitoring cell fractionation by western blotting for GAPDH (cytoplasmic marker), vimentin (cytoskeletal marker) and plectin confirmed the successful preparation of cytoskeletal fractions (CS) (Fig. 5A, lanes 1-12, 19-30). Plectin as well as filamentous actin (F-actin) were found enriched in the cytoskeletal fraction (Fig. 5A, lanes 6, 12, 24, 30). When plectin was immunoprecipitated from the cytoskeletal fractions followed by western blotting, vimentin as well as actin co-immunoprecipitated with plectin (Fig. 5A, lanes 13-18, 31-36), indicating that plectin binds

to both vimentin and F-actin in the actin cytoskeleton of invasive bladder cancer YTS-1 and Patient 3 cells. In addition, when vimentin was immunoprecipitated, plectin and actin co-immunoprecipitated with vimentin (Fig. 5A, lanes 19-24,37-42). These results taken together results indicate that a complex containing vimentin, plectin and F-actin is formed in invasive bladder cancer cells (Fig. 5A).

Numerous puncta where F-actin and cortactin (an invadopodium marker) co-localize were observed in YTS-1 cells (Fig. 6) (Sutoh et al., 2010) and the degradation of Matrigel by the F-actin-based structures was also observed in YTS-1 cells (Sutoh et al., 2010), indicating that YTS-1 has a high ability to form invadopodia. Cells were then analyzed by confocal microscopy for the spatial correlation between vimentin, plectin and F-actin core of invadopodia. YTS-1 cells were triple-stained with phalloidin (red), anti-vimentin (green) and anti-plectin (magenta) (Fig. 5B). Phalloidin staining visualized invadopodia as F-actin puncta (Fig. 5B, F-actin panels). Pairs of white arrows in the XY images indicate the points of the XY images projected to generate the Z-section images. Focusing on several typical invadopodia, the Z-section images of each staining were shown in the insets. We observed that YTS-1 cells form the downwardly-protruding typical invadopodia (Fig. 5B, F-actin panel, inset) (Fig. 7). White indicates the co-localization of plectin, vimentin and F-actin in the merged images. The white areas were seen at the base of the invadopodia in the merged Z-section images, indicating that plectin (magenta) and vimentin (green) co-localized at the base of the invadopodium (red) (Fig.

5B, insets) (Fig. 7). These results taken together with the co-immunoprecipitation results (Fig. 5A) indicate that vimentin, plectin and F-actin co-localized and formed a complex at the base of invadopodia. We found that plectin and vimentin co-localized at the base of the invadopodia in Patient 3 cell as well as YTS-1 (Fig. 5B; Fig. 7), suggesting that this is a physiologically relevant phenomenon in invasive bladder cancer cells.

The vimentin IF-plectin-invadopodia F-actin link is critical for invadopodia formation

To determine the role of plectin in the formation of the complex with vimentin, plectin and F-actin, we prepared plectin knockdown cells by establishing several YTS-1 cell lines expressing siRNA for plectin. The results from two representative cell lines (designated PIKD-1 and PIKD-2) were shown in this study. We also established a YTS-1 cell line expressing non-targeting siRNA as a control (designated YTS control). The expression level of plectin was decreased in both PIKD-1 and PIKD-2 cells without affecting the expression of vimentin, but the expression level of plectin in YTS control cells was equivalent to that in YTS-1 parent cells (Fig. 8). In the cytoskeletal fractions from PIKD-1 cells, plectin was almost undetectable and the amount of F-actin was slightly decreased (Fig. 9A, lanes 5 and 8). When vimentin was immunoprecipitated from the cytoskeletal fractions of YTS control cells, both plectin and actin were co-immunoprecipitated (Fig. 9A, lanes 11, 13, 15). However, actin was undetected in the

immunoprecipitates from PIKD-1 cells (Fig. 9A, lane 21), indicating that the vimentin IF binds to invadopodia F-actin via plectin. These results taken together with the co-immunoprecipitation results (Fig. 5A) strongly suggest that plectin anchors invadopodia to the vimentin IF network by crosslinking F-actin of invadopodia with vimentin IF.

The vimentin IF-plectin-invadopodia F-actin link was disrupted due to plectin knockdown without affecting the network formation of vimentin (Fig. 9A) (Fig. 10). To determine the role of the vimentin IF-plectin-invadopodia F-actin link in invadopodia formation, we examined invadopodia formation in plectin knockdown cells. The abilities of PIKD-1 and PIKD-2 cells to form invadopodia were significantly lower than YTS control cells (Fig. 9B). Cells were then triple-stained with anti-plectin (magenta), phalloidin (red) and anti-cortactin (green) for invadopodia formation. Invadopodia were visualized as yellow F-actin puncta, since cortactin is an invadopodia marker (Oser et al., 2009). YTS control cells show a typical cytosolic staining of plectin and formed numerous invadopodia (Fig. 9C, panels 1 and 2). In contrast, few obvious invadopodia were observed in PIKD-1 and PIKD-2 (Fig. 9C, panels 4 and 6). This is consistent with the observation that the amount of F-actin in the cytoskeletal fraction from PIKD-1 cells was decreased (Fig. 9A, lane 8). The panels 1-6 of Fig. 9C suggest that plectin expression is necessary for the invadopodia formation.

We checked the expression of plectin isoforms (1, 1k, 1f and 1d) focusing on the ones whose expression was observed in invasive cancer cells (McInroy and Määttä, 2011). We confirmed

that the plectin isoforms, 1, 1f and 1k which are the major crosslinker isoforms between intermediate filaments were expressed in YTS-1 cells (Fig. 11). Among them, plectin 1f was shown to crosslink vimentin IF with focal adhesion (FA), an actin cytoskeleton-associating adhesion structure, resulting in the stabilization of FA (Burgstaller et al., 2010). We then transfected PIKD-1 cells with a cDNA plasmid encoding a full-length version of mouse plectin (isoform 1f) (Reznicek et al., 2003) and established a stable cell line expressing mouse plectin in PIKD-1 (designated PIKD-1+mPl). Western blots showed that PIKD-1+mPl cells expressed mouse plectin at a level similar to that of endogenous plectin in YTS control cells (Fig. 9A, lane 6). Both mouse plectin and actin co-immunoprecipitated with vimentin (Fig. 9A, lanes 23, 25, 27), indicating that mouse plectin 1f crosslinked vimentin with F-actin and that the vimentin IF-plectin-invadopodia F-actin link was reconstituted in PIKD-1+mPl cells. The ability of PIKD-1+mPl cells to form invadopodia was restored (Fig. 9B) and numbers of typical invadopodia were observed in PIKD-1+mPl cells (Fig. 9C, panel 8). The rescue of impaired invadopodia formation by the re-expression of mouse plectin suggested that the anchorage of invadopodia to vimentin IF by plectin is required for invadopodia formation (Fig. 9).

To assess the importance of the vimentin IF-plectin-invadopodia F-actin link in invadopodia formation in a more specific manner, we blocked F-actin binding to plectin in cells. We established several stable cell lines expressing a FLAG-tagged actin binding domain (ABD) fragment of plectin (residues 1-428) (McLean et al., 1996). This domain was identified to be

responsible for actin binding (Garcia-Alvarez et al., 2003; Geerts et al., 1999). One representative clone was designated YTS+ABD. As a control, we also prepared a clone transfected with the FLAG vector alone (designated YTS mock). The expression of the ABD fragment barely affected the expression levels of plectin, vimentin and actin (Fig. 12A, lanes 1-8). The amount of plectin and vimentin in the cytoskeletal fractions were also unaffected by the ABD fragment, although the amount of F-actin in the cytoskeletal fraction was slightly decreased (Fig. 12A, lanes 9-14). While both vimentin and actin co-immunoprecipitated with plectin from the cytoskeletal fraction of YTS mock cells, only a comparatively small amount of actin co-immunoprecipitated with plectin in the case of YTS+ABD cells (Fig. 12A, lanes 17-20). This indicates that F-actin binding to plectin in YTS+ABD cells was indeed blocked by the ABD fragment, whereas vimentin binding to plectin was unaffected. Cells were triple-stained with anti-plectin (magenta), phalloidin (red) and anti-cortactin (green). The ability of YTS+ABD cells to form invadopodia was significantly lower than that of YTS mock cells (Fig. 12B). There was no difference in plectin expression between YTS mock and YTS+ABD cells (Fig. 12C, panels 1 and 3). Nevertheless, numerous invadopodia were observed in YTS mock cells, but only a small number, if any, in YTS+ABD cells (Fig. 12C, panels 2 and 4). This confirms the important role of F-actin binding to plectin in invadopodia formation. This result taken together with the results from Fig. 9 strongly suggests that the anchorage of invadopodia to vimentin IF by plectin is a critical molecular step for invadopodia formation.

The vimentin IF-plectin-invadopodia F-actin link is essential for cancer cell invasiveness

Invadopodia are required for the degradation of the ECM. Invadopodia formation enables cancer cells to invade surrounding tissues (Buccione et al., 2009; Murphy and Courtneidge, 2011). To determine if the vimentin IF-plectin-invadopodia F-actin link is essential for the invadopodia functions (degradation and migration), we tested if the disruption of this link affects invasiveness of cancer cells. We placed cells on Alexa Fluor 488-labelled Matrigel (green) for 2 h and then stained with Alexa Fluor 568-labelled phalloidin (red). YTS control cells formed the downwardly-protruding invadopodia (red) and that Matrigel (green) degradation occurred underneath the cells body (Fig. 13A, panel 1). In contrast, plectin knockdown cells formed no obvious invadopodia and little Matrigel degradation was observed (Fig. 13A, panels 2 and 3), whereas PIKD-1+mPl cells formed functional invadopodia that were capable of the Matrigel degradation (Fig. 13A, panel 4). In a Matrigel invasion assay, both PIKD-1 and PIKD-2 cells showed a significant reduction of their Matrigel invasion capacity and the invasion was restored in PIKD-1+mPl cells (Fig. 13B). In addition, YTS+ABD cells showed little Matrigel degradation (Fig. 13A, panels 5 and 6) and their invasiveness through Matrigel was reduced to a level similar to that of plectin knockdown cells (Fig. 13C). We assayed those YTS-derived cell lines for the secretion of matrix-metalloproteinase (MMP), since the MMP secretion is one of the important functions of invadopodia. We detected the MMP secretion from the cells with an

ability to form invadopodia (YTS control, PIKD-1+mPl, YTS mock cells). However, we detected only lower levels of MMP secretion from plectin knockdown cells (PIKD-1 and PIKD-2) and YTS+ABD cells with the lower ability to form invadopodia than YTS control and YTS mock cells, respectively (Fig. 2). These results taken together suggest that the anchorage of invadopodia to vimentin IF by plectin plays an essential role in ECM degradation and *in vitro* invasiveness through the invadopodia formation.

Cancer cell extravasation is the process whereby cancer cells exit the blood vessels to invade across endothelium into the tissues of a secondary organ site. Transendothelial migration mimics the migration of cancer cells through the endothelial cells. Matrigel Matrix invasion represents the degradation of basement membrane by cancer cells, since Matrigel Matrix consists of the components of the basement membrane. Therefore, how well cancer cells extravasate from the blood vessels can be evaluated by measuring the transendothelial migration plus Matrigel Matrix invasion capacities (Drake et al., 2009; Sugiyama et al., 2013). To determine the role of the anchorage of invadopodia to vimentin IF by plectin in transendothelial migration, we assayed the migration of cells through a monolayer of primary human endothelial cells from lung (HMVEC-L) (Transendothelial migration assay) (Fig. 14A, B). Transendothelial migration capacity of PIKD-1 and PIKD-2 was significantly lower than that of YTS control cells; further, the re-expression of mouse plectin in plectin knockdown cells restored transendothelial migration. Blocking of F-actin binding to plectin also reduced

transendothelial migration (Fig. 15A, YTS+ABD cells). These results indicate that the anchorage of invadopodia to vimentin IF by plectin is required for *in vitro* invasion capacity through the endothelial cell monolayer. These results taken together with Fig. 13B and C strongly suggest that the anchorage of invadopodia to vimentin IF by plectin is necessary for cancer cell extravasation.

To evaluate the role of the anchorage of invadopodia to vimentin IF by plectin in metastasis, we subjected those YTS-derived cell lines to a lung metastasis assay. Three weeks after the injection of the cells into the mouse tail vein, sections of mouse lungs were prepared and stained with Hematoxylin and Eosin (HE staining) (Fig. 15B-G) (Fig. 14C). The metastasized tumour area was determined by HE staining combined with anti-human uroplakin III (human bladder cancer marker) (Amin, 2009) staining (Fig. 16). When YTS control cells were injected, all the mice had lung metastases ($n = 5$), and their degree of metastasis was 58% (Fig. 15C and H). In contrast, none of the mice received the injection of PlKD-1 cells showed detectable metastases ($n = 7$) (Fig. 15D and H), and only 2 out of 6 mice injected with PlKD-2 cells showed a low degree of metastasis (0.71%) (Fig. 15E and H). These results indicate that lung metastasis was significantly reduced in plectin knockdown cells compared with control. Five out of 7 mice received PlKD-1+mPl cell injections showed lung metastasis with the degree of metastasis restored to 34.2% (Fig. 15F and H), indicating that re-expression of plectin significantly recovered lung metastasis. Mice injected with YTS+ABD cells significantly showed reduced

lung metastases with a degree of metastasis of 6.8% (Fig. 15G and H). These results indicate that the anchorage of invadopodia to vimentin IF by plectin is required for tumour formation in the lung of nude mice. This type of assay closely mimics haematogenous metastatic process including extravasation, invasion and colonization (Hatakeyama et al., 2010; Tsuboi et al., 2011). There was no significant difference in growth rate between YTS control, PIKD-1, PIKD-2 and YTS+ABD cell lines (Fig. 17). Nevertheless, plectin knockdown cells and YTS+ABD cells exhibited significantly lower lung metastasis than YTS control cells (Fig. 15H). This suggests that the lower metastasis is due to reduced extravasation and invasion into the lung tissues. These tumour formation data taken together with the results of Matrigel Matrix invasion and transendothelial migration strongly suggest that the anchorage of invadopodia to vimentin IF by plectin in bladder cancer cells is a critical molecular step for extravasation and invasion into lung tissues (Fig. 15).

Role of vimentin IF in invadopodia formation

We next asked what role vimentin IF plays in invadopodia formation. To address this question, we firstly examined the effect of silencing vimentin expression by shRNA on invadopodia formation. We prepared several stable YTS-1 cell lines with reduced vimentin

expression (Fig. 18A). In the cytoskeletal fraction from one of the vimentin knockdown cell lines (designated ViKD-1 cells), the amount of vimentin was reduced, but the amounts of plectin and actin were equivalent to those in the cytoskeletal fraction from YTS control cells (Fig. 19A, lanes 1,2,4,5,7 and 8). When plectin was immunoprecipitated, no vimentin was detected in the plectin immunoprecipitates, although actin was detected (Fig. 19A, lanes 10-21), indicating that plectin interacts with F-actin but that little interaction of plectin with vimentin occurred in ViKD-1 cells due to vimentin knockdown. The ability of ViKD-1 cells to form invadopodia was markedly reduced (Fig. 19B), suggesting that the vimentin expression is necessary for the invadopodia formation. We established a stable cell line expressing mouse vimentin in ViKD-1 cells (designated ViKD-1+mV). Mouse vimentin was expressed (Fig. 19A, lane 6) and the vimentin-plectin-invadopodia F-actin link was reconstituted in ViKD-1+mV cells (Fig. 19A, lanes 22-27). The ability of ViKD-1+mV cells to form invadopodia was restored (Fig. 19B). These results suggest that the vimentin expression is required for invadopodia formation.

To determine whether the vimentin assembly into the filament is important for invadopodia formation, we disrupted the filament assembly of endogenous vimentin and examined the effect of this disruption on invadopodia formation. We prepared a stable cell line expressing a FLAG-tagged dominant negative mutant of vimentin (residues 1-136) (designated YTS+VDN). It has been demonstrated that the N-terminal fragment of vimentin lacking the tail region

effectively functions as a dominant negative disrupter of vimentin IF assembly, since this fragment lacks any of the tail sequence essential for the filament assembly of vimentin (Kural et al., 2007; Whipple et al., 2008). The expression of this construct disrupts vimentin IF without affecting the vimentin expression and other cytoskeletal structures (Chang et al., 2009; Kural et al., 2007; Mendez et al., 2010). In YTS+VDN cells, endogenous vimentin was expressed at the similar level to a control YTS cells (YTS mock) (Fig. 19C, lane 4) and vimentin co-immunoprecipitated with plectin (Fig. 19C, lane 18), indicating that the expression of this dominant negative vimentin mutant affected neither endogenous vimentin expression nor vimentin binding to plectin. Nevertheless, the ability of YTS+VDN cells to form invadopodia was remarkably reduced (Fig. 19D), indicating that the assembly of vimentin into the filament is critical for the invadopodia formation. We then examined each cell line by confocal microscopy for the spatial correlation between vimentin and invadopodium. Cells were double-stained with anti-vimentin (green) and phalloidin (red) (Fig. 19E-H). Pairs of white arrows in the XY images indicate the points of the XY image projected to generate Z-section image. The Z-section images of each staining were shown in the insets. Endogenous vimentin IF formed an intricate network from the perinuclear region to the cell periphery in the XY-image of YTS control cell (Fig. 19E). The Z-section images showed that invadopodia were anchored to vimentin IF and that the invadopodia downwardly-protruded from the vimentin IF (Fig. 19E, inset). When the vimentin expression was knocked down, no vimentin IF network was observed and no

invadopodia were seen in both XY- and Z-section images of ViKD-1 cell (Fig. 19F). In a ViKD-1+mV cell, the vimentin IF network was reconstituted by the re-expression of mouse vimentin and numerous typical invadopodia anchored to vimentin IF were seen (Fig. 19G). When the endogenous vimentin IF was disrupted by the expression of the dominant negative vimentin fragment (YTS+VDN), vimentin aggregated near the nucleus and the peripheral cytoplasm was nearly devoid of filamentous vimentin (Fig. 19H). In YTS+VDN cells, neither vimentin IF nor typical invadopodia were observed (Fig. 19H). In addition, no downwardly-protruding typical invadopodia were observed in the Z-section image of YTS+VDN cells (Fig. 19H, inset). These results indicate that the vimentin expression is not sufficient and the vimentin assembly into the filament is required for the invadopodia formation (Fig. 19). This suggests that the vimentin IF network functions as a scaffold for invadopodia, thereby enabling invadopodia to stably elongate and protrude from this scaffold.

Discussion

In the present study, we have discovered a novel role that vimentin IF and plectin play in the cancer cell invasion process. From the results shown in Figs. 5, 9, 12, 13, 15, and 19, we concluded that vimentin IF and plectin provide a scaffold for invadopodia and this scaffolding is required for invadopodia formation, matrix degradation and invasiveness. The N-terminal region of plectin binds to the F-actin core of invadopodia and its C-terminal region binds to the vimentin IF network, resulting in anchorage of invadopodia to vimentin IF. This anchorage scaffolds and stabilizes invadopodia, enabling invadopodia to stably elongate and protrude in invasive cancer cells. The functional invadopodia facilitate transendothelial migration, leading to cancer cell extravasation and metastasis. It has been demonstrated that plectin and vimentin IF play an essential role in cancer cell invasion (Kidd et al., 2014; McInroy and Maatta, 2011). In addition, it has been pointed out the importance of the plectin-vimentin IF interaction in the regulation of the cytoskeletal architectures in other types of cells (Brown et al., 2001; Favre et al., 2011). However, the mechanism by which the plectin-vimentin IF interaction functions in the invasion process has not been understood. We have shown a specific role of the plectin-vimentin IF interaction in metastatic process of invasive cancer cells.

The formation of vimentin IF is initiated during the epithelial to mesenchymal transition (EMT) that takes place during embryogenesis, tumorigenesis and metastasis (Hay, 2005).

Vimentin IF induces changes in cell shape, motility and adhesion of cancer cells, resulting in the promotion of cancer cell invasion (Mendez et al., 2010). The vimentin expression is a marker of invasive potential and a predictor of poor patient prognosis in many cancers (Hugo et al., 2007; Lang et al., 2002). However, the detailed molecular mechanisms underlying the promotion of cancer invasion by vimentin were not fully understood. On the other hand, plectin binds to the $\beta 4$ cytoplasmic tail of the $\alpha 6\beta 4$ integrin and cytokeratin IF to constitute hemidesmosome (HD) that mediates stable anchoring of the cell to ECM in epithelial cells (Koster et al., 2004), but plectin dissociates from the $\beta 4$ cytoplasmic tail and HD disassembles during EMT in several types of cancer (Kokkinos et al., 2007; Litjens et al., 2006; Takkunen et al., 2006). In addition, it has been recently reported that the plectin expression is increased in many cancer cells and that plectin is thought to play an important role in the promotion of cancer cell invasion (Bausch et al., 2011; Katada et al., 2012; McInroy and Maatta, 2011). However, what plectin interacts with after the disassembly of HD during EMT was not known and what roles plectin plays in invasion process were not understood, either. Our results revealed that invasive cancer cells form the vimentin IF-plectin-invadopodia F-actin link to provide a scaffold for functional invadopodia. If vimentin IF is absent from this vimentin IF-plectin-invadopodia F-actin architecture, invadopodia lose the scaffold. If plectin is absent, invadopodia lose the anchorage to the scaffold. We demonstrated that invadopodia formation is impaired in either case. Presumably, the EMT-experienced invasive cancer cells up-regulate the expression of vimentin

IF and plectin, forming the vimentin IF-plectin-invadopodia F-actin link and contributing to the formation of functional invadopodia.

Studies on invadosomes (invadopodia/podosomes) have so far made a great progress by focusing on the mechanisms regulating their actin cytoskeleton (Garcia et al., 2012; Linder, 2009; Linder et al., 1999; Oser et al., 2009) and signalling pathways mediating their formation (Murphy and Courtneidge, 2011; Seals et al., 2005). However, little has been revealed about how cells provide a scaffold for such huge and dynamic F-actin-based structures. On the other hand, Schoumacher and colleagues reported that vimentin is localized at the base of invadopodia and that vimentin IF is required for invadopodia elongation (Schoumacher et al., 2010). However, how invadopodia are associated with vimentin IF in cells remained to be determined. In this study, we demonstrated that plectin plays a critical role in providing a scaffold for invadopodia by anchoring these structures to vimentin IF and that this scaffolding is actually required for cancer cell invasion and extravasation for metastasis.

The phenotypic difference in the ability to form invadopodia between KK-47 and KK-47HM4 cells is a result of complex changes in gene expression. Our analysis of the gene expression profile showed that the increased expression of vimentin and plectin is associated with highly invasive phenotypes. Such invasive phenotypes should involve the changes in the expression of numbers of genes besides vimentin and plectin. In fact, it has been reported that several transcription factors such as Twist1 are involved in invasive phenotypes including

invadopodia formation (Eckert et al., 2011). In the future, the functions of those genes involved in invasive phenotypes will be elucidated.

Podosomes which are formed by leukocytes and homologous membrane structures with invadopodia are required for transendothelial migration during leukocyte extravasation and recruitment to inflamed sites (Carman et al., 2007; Carman and Springer, 2008). Considering this podosome function, it seems plausible that invadopodia contribute to transendothelial migration during cancer cell extravasation for metastasis. A growing body of evidence has recently supported the crucial roles of invadosomes (invadopodia/podosomes) *in vivo* (Blouw et al., 2008; Gligorijevic et al., 2012; Linder et al., 1999; Quintavalle et al., 2010; Weaver, 2008). Particularly, Gligorijevic and colleagues have recently demonstrated that invadopodia formation is required for cancer cell intravasation in an *in vivo* system (Gligorijevic et al., 2012). We also showed that impaired invadopodia formation results in reduced transendothelial migration and lung metastasis of invasive bladder cancer cells using the animal model (Fig. 15) (Tokui et al., 2014). Our results strongly suggest that invadopodia formation is required for cancer cell extravasation by facilitating transendothelial migration. Our investigation thus provides a new insight into the roles of vimentin IF and plectin in invasive cancer cells and unveils a critical molecular process for cancer cell invasion and extravasation for metastasis.

Acknowledgements

We thank Mr. K. Tone (Hirosaki University School of Medicine and Hospital), Ms. M. Yamaguchi and Mr. K. Harada (Carl Zeiss) for expert technical support. This study was supported by the Grants-in-Aid for Scientific Research from the Japanese Society for the Promotion of Science (22570131) (to S.T.), (B22390301) (to C.O. and S.T.), (24659708) (to C.O.) and Austrian Science Research Fund grant I413-B09 (part of Multilocation DFG-Research Unit 1228) (to G.W.).

References

- Amin MB, Histological variants of urothelial carcinoma: diagnostic, therapeutic and prognostic implications. *Mod Pathol*. 2009; 22 Suppl 2: S96-S118.
- Ayala I, Baldassarre M, Giacchetti, G, et al. Multiple regulatory inputs converge on cortactin to control invadopodia biogenesis and extracellular matrix degradation. *J Cell Sci*. 2008; 121: 369-378.
- Bausch D, Thomas S, Mino-Kenudson M, et al. Plectin-1 as a novel biomarker for pancreatic cancer. *Clin Cancer Res*. 2011; 17: 302-309.
- Blouw B, Seals DF, Pass I, et al. A role for the podosome/invadopodia scaffold protein Tks5 in tumor growth in vivo. *Eur J Cell Biol*. 2008; 87: 555-567.
- Brown MJ, Hallam JA, Liu Y, et al. Cutting edge: integration of human T lymphocyte cytoskeleton by the cytolinker plectin. *J Immunol*. 2001; 167: 641-645.
- Buccione R, Caldieri G, Ayala I, Invadopodia: specialized tumor cell structures for the focal degradation of the extracellular matrix. *Cancer Metastasis Rev*. 2009; 28: 137-149.
- Burgstaller G, Gregor M, Winter, L, et al. Keeping the vimentin network under control: cell-matrix adhesion-associated plectin 1f affects cell shape and polarity of fibroblasts. *Mol Biol Cell*. 2010; 21: 3362-3375.

Carman CV, Sage PT, Sciuto TE, et al. Transcellular diapedesis is initiated by invasive podosomes. *Immunity*. 2007; 26: 784-797.

Carman CV, Springer TA, Trans-cellular migration: cell-cell contacts get intimate. *Curr Opin Cell Biol*. 2008; 20: 533-540.

Chang L, Barlan K, Chou YH, et al. The dynamic properties of intermediate filaments during organelle transport. *J Cell Sci*. 2009; 122: 2914-2923.

Clark EA, Golub TR, Lander ES, et al. Genomic analysis of metastasis reveals an essential role for Rho C. *Nature*. 2000; 406: 532-535.

Drake JM, Strohhahn G, Bair TB, et al. Moreland, ZEB1 enhances transendothelial migration and represses the epithelial phenotype of prostate cancer cells. *Mol Biol Cell*. 2009; 20: 2207-2217.

Eckert MA, Lwin TM, Chang AT, et al. Twist1-induced invadopodia formation promotes tumor metastasis. *Cancer Cell*. 2011; 19: 372-386.

Even-Ram S, Yamada KM, Cell migration in 3D matrix. *Curr Opin Cell Biol*. 2005; 17: 524-532.

Favre B, Schneider Y, Lingasamy P, et al. Plectin interacts with the rod domain of type III intermediate filament proteins desmin and vimentin. *Eur J Cell Biol*. 2011; 90: 390-400.

Garcia-Alvarez B, Bobkov A, Sonnenberg A, et al. Structural and functional analysis of the actin binding domain of plectin suggests alternative mechanisms for binding to F-actin and integrin $\beta 4$. *Structure*. 2003; 11: 615-625.

Garcia E, Jones GE, Machesky LM, et al. WIP: WASP-interacting proteins at invadopodia and podosomes. *Eur J Cell Biol*. 2012; 91: 869-877.

Geerts D, Fontao L, Nievers MG, et al. Binding of integrin $\alpha 6\beta 4$ to plectin prevents plectin association with F-actin but does not interfere with intermediate filament binding. *J Cell Biol*. 1999; 147: 417-434.

Gligorijevic B, Wyckoff J, Yamaguchi H, et al. N-WASP-mediated invadopodium formation is involved in intravasation and lung metastasis of mammary tumors. *J Cell Sci*. 2012; 125: 724-734.

Gupta GP, Massague J, Cancer metastasis: building a framework. *Cell* 2006; 127: 679-695.

Hatakeyama S, Yamamoto H, Ohyama C, Tumor formation assays. *Methods Enzymol*. 2010; 479: 397-411.

Hay ED, The mesenchymal cell, its role in the embryo, and the remarkable signaling mechanisms that create it. *Dev Dyn*. 233, 706-720.

Hisazumi H, Uchibayashi T, Katoh M, et al. 1981. Anticancer drug sensitivity in vitro in the bladder cancer cell line, KK-47 and prophylactic use of carbazilquinone and urokinase in bladder cancer. *Urol Res* . 1981; 9: 231-235.

Hugo H, Ackland ML, Blick T, et al. Epithelial--mesenchymal and mesenchymal--epithelial transitions in carcinoma progression. *J of Cell Physiol.* 2007; 213: 374-383.

Ivaska J, Pallari HM, Nevo J, et al. Novel functions of vimentin in cell adhesion, migration, and signaling. *Exp Cell Res.* 2007; 313: 2050-2062.

Jaffe AB, Hall A, Rho GTPases in transformation and metastasis. *Advances in Cancer Res.* 2002; 84: 57-80.

Katada K, Tomonaga T, Satoh M, et al. Plectin promotes migration and invasion of cancer cells and is a novel prognostic marker for head and neck squamous cell carcinoma. *J Proteomics.* 2012; 75: 1803-1815.

Kayajima T, Shirahama T, Yanase I, et al. Characterization of a new cell line established from a human urinary-bladder cancer, with special reference to metastatic ability to the lung. *Jpn J Urol Surg.* 1989; 2: 577-580.

Kidd ME, Shumaker DK, Ridge KM, The role of vimentin intermediate filaments in the progression of lung cancer. *Am J Respir Cell Mol Biol.* 2014;50: 1-6.

Kokkinos MI, Wafai R, Wong MK, et al. Vimentin and epithelial-mesenchymal transition in human breast cancer--observations in vitro and in vivo. *Cells Tissues Organs.* 2007; 185: 191-203.

Koster J, van Wilpe S, Kuikman I, et al. Role of binding of plectin to the integrin beta4 subunit in the assembly of hemidesmosomes. *Mol Biol Cell.* 2004; 15: 1211-1223.

Kubota Y, Nakada T, Yanai H, et al. Electroporation in bladder cancer chemotherapy. *Cancer Chemother Pharmacol.* 1996; 39: 67-70.

Kural C, Serpinskaya AS, Chou YH, et al. Tracking melanosomes inside a cell to study molecular motors and their interaction. *Proc Natl Acad Sci U. S. A.* 2007; 104: 5378-5382.

Lang SH, Hyde C, Reid IN, et al. Enhanced expression of vimentin in motile prostate cell lines and in poorly differentiated and metastatic prostate carcinoma. *Prostate* 2002; 52: 253-263.

Linder S, Invadosomes at a glance. *J Cell Sci.* 2009; 122: 3009-3013.

Linder S, Nelson D, Weiss M, et al. Wiskott-Aldrich syndrome protein regulates podosomes in primary human macrophages. *Proc Natl Acad of Sci U. S. A.* 1999; 96: 9648-9653.

Litjens SH, de Pereda JM, Sonnenberg A., Current insights into the formation and breakdown of hemidesmosomes. *Trends Cell Biol.* 2006; 16: 376-383.

McInroy L, Määttä A, Plectin regulates invasiveness of SW480 colon carcinoma cells and is targeted to podosome-like adhesions in an isoform-specific manner. *Exp Cell Res.* 2011; 317: 2468-2478.

McLean WH, Pulkkinen L, Smith FJ, et al. Loss of plectin causes epidermolysis bullosa with muscular dystrophy: cDNA cloning and genomic organization. *Genes Dev.* 1996; 10: 1724-1735.

Mendez MG, Kojima S, Goldman RD, Vimentin induces changes in cell shape, motility, and adhesion during the epithelial to mesenchymal transition. *FASEB J.* 2010; 24: 1838-1851.

Murphy DA, Courtneidge SA, The 'ins' and 'outs' of podosomes and invadopodia: characteristics, formation and function. *Nat Rev Mol Cell Biol.* 2011; 12: 413-426.

Oser M, Yamaguchi H, Mader CC, et al. Cortactin regulates cofilin and N-WASp activities to control the stages of invadopodium assembly and maturation. *J Cell Biol.* 2009; 186: 571-587.

Quintavalle M, Elia L, Condorelli G, et al. MicroRNA control of podosome formation in vascular smooth muscle cells in vivo and in vitro. *J Cell Biol.* 2010; 189: 13-22.

Rezniczek GA, Abrahamsberg C, Fuchs P, et al. Plectin 5'-transcript diversity: short alternative sequences determine stability of gene products, initiation of translation and subcellular localization of isoforms. *Hum Mol Genet.* 2003; 12: 3181-3194.

Satelli A, Li S, Vimentin in cancer and its potential as a molecular target for cancer therapy. *Cell Mol Life Sci.* 2011; 68: 3033-3046.

Schoumacher M, Goldman RD, Louvard, D, et al. Actin, microtubules, and vimentin intermediate filaments cooperate for elongation of invadopodia. *J Cell Biol.* 2010; 189: 541-556.

Seals DF, Azucena EF Jr, Pass I, et al. 2005. The adaptor protein Tks5/Fish is required for podosome formation and function, and for the protease-driven invasion of cancer cells. *Cancer Cell.* 2005; 7: 155-165.

Smith SC, Nicholson B, Nitz M, et al. Profiling bladder cancer organ site-specific metastasis identifies LAMC2 as a novel biomarker of hematogenous dissemination. *Am J Pathol.* 2009; 174: 371-379.

Sugiyama N, Yoneyama MS, Hatakeyama S, et al. In vivo selection of high-metastatic subline of bladder cancer cell and its characterization. *Oncol Res.* 2013; 20: 289–295.

Sutoh M, Hashimoto Y, Yoneyama T, et al. Invadopodia formation by bladder tumor cells. *Oncol Res.* 2010; 19: 85-92.

Takkunen M, Grenman R, Hukkanen M, et al. Snail-dependent and -independent epithelial-mesenchymal transition in oral squamous carcinoma cells. *J Histochem Cytochem.* 2006; 54: 1263-1275.

Tokui N, Yoneyama MS, Hatakeyama S, et al. Extravasation during bladder cancer metastasis requires cortactin-mediated invadopodia formation. *Mol Med Rep.* 2014; 9: 1142-1146.

Tsuboi S, Sutoh M, Hatakeyama S, et al. A novel strategy for evasion of NK cell immunity by tumours expressing core2 O-glycans. *EMBO J.* 2011; 30: 3173-3185.

Weaver AM, Cortactin in tumor invasiveness. *Cancer Lett.* 2008; 265: 157-166.

Whipple RA, Balzer EM, Cho EH, et al. Vimentin filaments support extension of tubulin-based microtentacles in detached breast tumor cells. *Cancer Res.* 2008; 68: 5678-5688.

Wiche G, Winter L, Plectin isoforms as organizers of intermediate filament cytoarchitecture. *Bioarchitecture.* 2011; 1: 14-20.

Winter L, Wiche G, The many faces of plectin and plectinopathies: pathology and mechanisms.

Acta Neuropathol 2013; 125: 77-93.

Yamamoto H, Sutoh M, Hatakeyama S, et al. Requirement for FBP17 in invadopodia formation

by invasive bladder tumor cells. J Urol. 2011; 85: 1930-1938.

Figure Legends

Fig. 1. Invadopodia formation and increased expression of vimentin and plectin in invasive bladder cancer cells. (A and B) Invadopodia formation in KK-47 (A) and KK-47HM4 cells (B) was analyzed by confocal laser scanning microscopy. Cells were double-stained with phalloidin (left panels) and anti-cortactin (invadopodium marker) (middle panels). The merged images were shown (right panels). *Yellow* indicates co-localization in the merged images. Invadopodia are visualized in the KK-47HM4 cell as puncta where F-actin and cortactin co-localize (B, right panels). Several typical invadopodia were indicated by white arrows. Bar, 20 μm . (C) Invadopodia formation of bladder cancer cell lines. The percentage of the cells with invadopodia was scored (total 200 cells) in 3 randomly selected fields. Data represent mean \pm s.d. of triplicate measurements. (D) Matrigel degradation by KK-47HM4 cells. Cells were placed on the Alexa Fluor 488-labelled Matrigel for 2 h, stained with Alexa Fluor 568-labelled phalloidin for invadopodia and then examined by confocal microscopy. Upper panels are the XY-images and lower panels are the Z-section images. F-actin (red) and Matrigel (green) were visualized in the left and middle panels, respectively. The merged images are shown in the right panels. Bar, 20 μm . (E) Domain organizations of vimentin and plectin. Human vimentin (466 amino acids) is constituted by a globular N-terminal head, coiled-coil domain and C-terminal tail. Human plectin (4574 amino acids) is composed of three main sections; a central rod

domain (Rod), the N-terminal region and C-terminal region. The C-terminal region contains six sequence repeats. Repeats one to five show a sequence similarity with plakin repeat domain B (B) and the C-terminal repeat is a plakin repeat domain C (C). The vimentin binding domain (VBD) resides within the fifth plakin repeat domain B. The N-terminal domain contains the actin binding domain (ABD). (F) Western blots for the expression levels of plectin, vimentin, actin and GAPDH in bladder cancer cells. Six bladder cancer cell lines were used: the non-invasive bladder cancer cells, KK-47, RT-4 and 5637 and the invasive bladder cancer cells, T24, BOY and YTS-1. Primary culture cells from three bladder cancer patients were used: Patient 1 (non-invasive), Patient 2 and 3 (invasive).

Fig. 2. Secretion of matrix metalloproteinase (MMP) from bladder cancer cells. Conditioned media were collected and assayed for gelatinase activity by zymography. Lane 1, MMP marker. Lanes 2-9, Pro-MMP-2 secretion from bladder cancer cells.

Fig. 3. Western blots for the expression levels of vimentin, plectin, actin and GAPDH in the different preparation of KK-47 and KK-47HM4 cells (lanes 1-8), and beta4 subunit and GAPDH in 5637 and YTS-1 cells (lanes 9-12).

Fig. 4. Profile of bladder cancer patients used in this study and invadopodia formation. **(A)** Profile of bladder cancer patients used in this study. pT, pathological stage. pTa, non-invasive; pT2 <, invasive. **(B)** The formation of invadopodia in patient primary culture cells was examined by immunofluorescence microscopy. Primary culture cells from Patient 1 (non-invasive) and Patient 3 (invasive) were stained with phalloidin. The arrows indicate typical invadopodia. Bar, 20 μ m. **(C)** Matrigel Matrix degradation by invadopodia formed in Patient 3 cells. Cells were placed on Alexa Fluor 488-labeled Matrigel for 2 hours. Upper and lower panels are confocal images showing XY and XZ sections, respectively. Bar, 20 μ m.

Fig. 5. Formation of the vimentin IF-plectin-invadopodia F-actin link in invasive cancer cells. **(A)** Subcellular fractionation of YTS-1 cells (lanes 1-12) and Patient 3 cells (lanes 19-30). Three fractions, Cytoplasmic fraction, C; nuclear fraction, N and cytoskeletal fraction, CS were prepared from the cells. Each fraction was analyzed by western blotting using anti-GAPDH (lanes 1-3, 19-21), anti-plectin (lanes 4-6, 22-24), anti-vimentin (lanes 7-9, 25-27) and anti-actin (lanes 10-12, 28-30). Plectin was immunoprecipitated from the cytoskeletal fractions of YTS-1 (lanes 13-18) and Patient 3 (lanes 31-36) cells. Anti-plectin, monoclonal antibody to plectin. IgG, Isotype-matched control IgG. Plectin immunoprecipitates were analyzed by western blotting for plectin (lanes 13, 14, 31, 32), vimentin (lanes 15, 16, 33, 34) and actin (lanes 17, 18, 35, 36). Vimentin was immunoprecipitated from the cytoskeletal fractions of YTS-1 (lanes

19-24) and Patient 3 (lanes 37-42) cells. Anti-vimentin, monoclonal antibody to vimentin. The vimentin immunoprecipitates were analysed by western blotting for plectin (lanes 19,20,37,38), vimentin (lanes 21,22,39,40) and actin (lanes 23,24,41,42). (B) Confocal laser scanning micrographs of YTS-1 (left panels) and Patient 3 cells (right panels). Cells were triple-stained with phalloidin (red), anti-vimentin (green) and anti-plectin (magenta). Pairs of white arrows in the XY-images indicate the points of the XY-images projected to generate the Z-section images. The Z-section images were shown in the insets. Bar, 20 μ m.

Fig. 6. Invadopodia formation in YTS-1. Cells were double-stained with phalloidin (left) and anti-cortactin (middle). The merged image was shown (right). Several typical invadopodia were indicated by white arrows. Bar, 20 μ m.

Fig. 7. The spatial correlation between vimentin, plectin and F-actin core of invadopodia in YTS-1 and Patient 3 cells. The Z-section images of each staining in YTS-1 (A) and Patient 3 (B) cells were shown. Bar, 5 μ m.

Fig. 8. Knockdown of plectin and re-expression of plectin in plectin knockdown cells. Total protein samples prepared from YTS-1 parent, YTS control, PlKD-1 and PlKD-2 cells were analysed by western blotting for the expression of plectin (lanes 1-4), vimentin (lanes 5-8), actin

(lanes 9-12) and GAPDH (lanes 13-16). The expression level of plectin was decreased in PIKD-1 and PIKD-2 (lanes 3, 4) without affecting the expression of vimentin, actin and GAPDH.

Fig. 9. Expression of plectin is required for invadopodia formation. (A) Occurrence of vimentin (lanes 1-3), plectin (lanes 4-6) and actin (lanes 7-9) in the cytoskeletal fraction (CS) from each cell line. Vimentin was immunoprecipitated from the cytoskeletal fractions of YTS control (lanes 10-15), PIKD-1 (lanes 16-21) and PIKD-1+mPl cells (lanes 22-27) followed by western blotting for vimentin, plectin and actin. Anti-vimentin, monoclonal antibody to vimentin. IgG, Isotype-matched control IgG. (B) Invadopodia formation of each cell line. The percentage of the cells with invadopodia was scored (total 200 cells) in 3 randomly selected fields. Data represent mean \pm s.d. of triplicate measurements. (C) Confocal laser scanning micrographs of YTS control (lanes 1, 2), PIKD-1 (panels 3, 4), PIKD-2 (panels 5, 6) and PIKD-1+mPl (panels 7, 8) cells. Cells were triple-stained with anti-plectin, phalloidin and anti-cortactin (invadopodium marker) and analyzed by confocal microscopy. Bar, 20 μ m.

Fig. 10. Vimentin IF in PIKD-1 cell. YTS control and PIKD-1 cells were double-stained with anti-plectin and anti-vimentin and analyzed by immunofluorescence microscopy. Bar, 20 μ m.

Fig. 11. Expression of plectin isoforms in YTS-1 cells. The expression levels of the major crosslinker isoforms between intermediate filaments were semiquantitatively compared on RT-PCR using the isoform-specific primers (McInroy, L. and Määttä, A, (2011) *Experimental Cell Research* 317:2468-2478). RT-PCR was undertaken using SuperScript III One-Step RT-PCR System with Platinum Taq DNA polymerase.

Fig. 12. F-actin binding to plectin is necessary for invadopodia formation. (A) Total protein samples were analyzed by western blotting for the expression of plectin (lanes 1, 2), vimentin (lanes 3, 4), actin (lanes 5, 6) and FLAG-tagged ABD fragment (lanes 7, 8). Occurrence of plectin (lanes 9, 10), vimentin (lanes 11, 12) and actin (lanes 13, 14) in the cytoskeletal fraction (CS) from each cell line. Plectin was immunoprecipitated from the cytoskeletal fractions followed by western blotting for plectin (lanes 15, 16), vimentin (lanes 17, 18) and actin (lanes 19, 20). Cells were transfected with vector alone (mock-transfected, designated YTS mock). A stable cell line expressing the FLAG-tagged ABD fragment containing plectin ABD region (+ABD, YTS+ABD cells). (B) Invadopodia formation of each cell line. The percentage of the cells with invadopodia was scored (total 200 cells) in 3 randomly selected fields. Data represent mean \pm s.d. of triplicate measurements. (C) Confocal laser scanning micrographs of YTS mock (panels 1, 2) and YTS+ABD (panels 3, 4) cells. Cells were triple-stained with anti-plectin, phalloidin and anti-cortactin and analyzed by confocal microscopy. Bar, 20 μ m.

Fig. 13. The vimentin IF-plectin-invadopodia F-actin link is essential for *in vitro* invasiveness.

(A) Matrigel degradation by YTS control (panel 1), PIKD-1 (panel 2), PIKD-2 (panel 3), PIKD-1+mP1 (panel 4), YTS mock (panel 5) and YTS+ABD cells (panel 6). Cells were placed on the Alexa Flour 488-labelled Matrigel for 2 h, stained with Alexa Fluor 568-labelled phalloidin for invadopodia and then examined by confocal microscopy. Matrigel degradation is visualized as a black hollow underneath the cell body formed by invadopodia (red) in Alexa Flour 488-labelled Matrigel (green) on confocal Z-section images. Bar, 20 μ m. (B and C) Matrigel invasion capacity of each cell line as measured by a Matrigel Matrix invasion assay system using the Boyden chamber. Data represent mean \pm s.d. of triplicate measurements.

Fig. 14. (A) A schematic drawing of *in vitro* transendothelial migration assay. (B) The monolayer of HMVEC-L cells grown on the top surface of the filter of the cell culture insert. We confirmed the integrity of the monolayer by measuring the permeability of FITC-dextran. Bar, 50 μ m. These figures were previously published (Sugiyama N, et al. (2013) *Oncology Research* 20: 289–295), but re-displayed here for readers. (C) A schematic drawing of the method to evaluate the degree of lung metastasis used in this study.

Fig. 15. The vimentin IF-plectin-invadopodia F-actin link is required for cancer cell extravasation. (A) *In vitro* transendothelial migration capacities of the YTS-1-derived cells. Migration through the endothelial cells from human lung microvessels was assayed. Data represent mean \pm s.d. of triplicate measurements. (B)-(G) Capacities of lung metastasis of the YTS-1-derived cells. Lung metastasis of mice that received the injection of medium only (B) and bladder cancer cells (C-G) was examined histologically. After three weeks of injection, lungs were removed and trisected and lung sections were prepared. The sections were stained with hematoxylin and eosin (HE). In upper panels, representative lung sections were photographed for evaluation of the degree of metastasis. Bar, 5 mm. The degree of metastasis was evaluated by the proportion (%) of the tumour area to the total lung area on the section (Supplementary Fig. S9C). Lower panels, the area of the lung sections indicated by arrows were examined at higher magnification. Bar, 0.2 mm. Tumour areas were confirmed by staining the serial sections with anti-human uroplakin III (human bladder cancer marker) antibody (Supplementary Fig. S10). (H) The degree of lung metastasis of each cell line was calculated. Data represent mean \pm s.d. Mann-Whitney *u*-test was used to assess statistical significance between two groups. Differences were considered significant, if $P < 0.05$.

Fig. 16. Lung tumour area of mouse that received the injection of YTS control cells. The serial sections of lung were stained with HE (left panel) and anti-human uroplakin III (human

bladder cancer cell marker). This is displayed as a typical example for mouse lung section stained with HE and anti-human uroplakin III antibody. Bar, 0.2 mm.

Fig. 17. Growth kinetics of YTS control, PIKD-1 and PIKD-2 cells were measured by using Cell Counting Kit-8 (Dojindo, Japan)

Fig. 18. Knockdown of vimentin and re-expression of vimentin in vimentin knockdown cells. Total protein samples prepared from each cell line was analysed by western blotting for the expression of vimentin (lanes 1-4), plectin (lanes 5-8), actin (lanes 9-12) and GAPDH (lanes 13-16).

Fig. 19. Assembly of vimentin into the filament is required for invadopodia formation. (A) Occurrence of plectin (lanes 1-3), vimentin (lanes 4-6) and actin (lanes 7-9) in the cytoskeletal fraction from each cell line. Plectin was immunoprecipitated from the cytoskeletal fraction of YTS control (lanes 10-15), ViKD-1 (lanes 16-21) and ViKD-1+mV cells (lanes 22-27) followed by western blotting for vimentin, plectin and actin. Anti-plectin, monoclonal antibody to plectin. IgG, Isotype-matched control IgG. (B) Invadopodia formation of each cell line (YTS control, ViKD-1, and ViKD+mV). The percentage of the cells with invadopodia was scored (total 200 cells) in 3 randomly selected fields. Data represent mean \pm s.d. of triplicate

measurements. (C) Total protein samples were analyzed by western blotting for the expression of plectin (lanes 1, 2), vimentin (lanes 3, 4), actin (lanes 5, 6) and FLAG-tagged a dominant negative vimentin fragment (VDN) (lanes 7, 8). Occurrence of plectin (lanes 9, 10), vimentin (lanes 11, 12) and actin (lanes 13, 14) in the cytoskeletal fraction (CS) from each cell line. Plectin was immunoprecipitated from the cytoskeletal fraction followed by western blotting for plectin (lanes 15, 16), vimentin (lanes 17, 18) and actin (lanes 19, 20). Cells were transfected with vector alone (mock-transfected, designated YTS mock). A stable cell line expressing FLAG-tagged VDN fragment containing vimentin N-terminal region to disassemble vimentin IF. (D) Invadopodia formation of each cell line (YTS mock and YTS+VDN). The percentage of the cells with invadopodia was scored (total 200 cells) in 3 randomly selected fields. Data represent mean \pm s.d. of triplicate measurements. (E)-(H) Confocal laser scanning micrographs of a YTS control, ViKD-1, ViKD-1+mV and YTS+VDN cell. Cells were double-stained with anti-vimentin (green) and phalloidin (red) and analyzed by confocal microscopy. Pairs of white arrows in the XY-images indicate the points of the XY-images projected to generate the Z-section images. The Z-section images were shown in the insets. Bar, 20 μ m.

Fig. 1

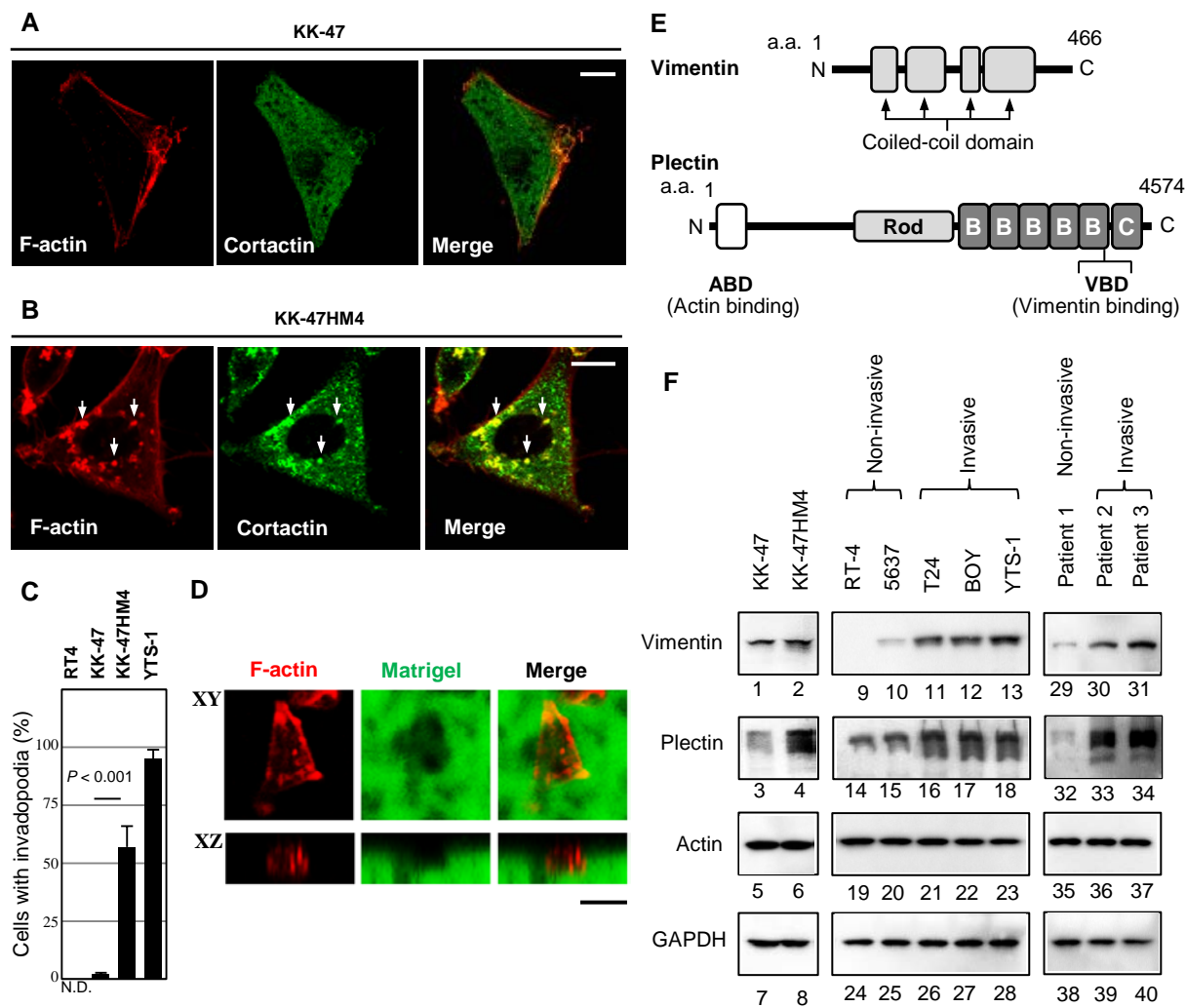


Fig. 2

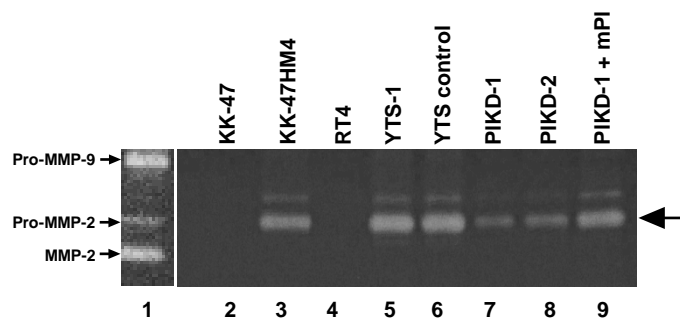


Fig. 3

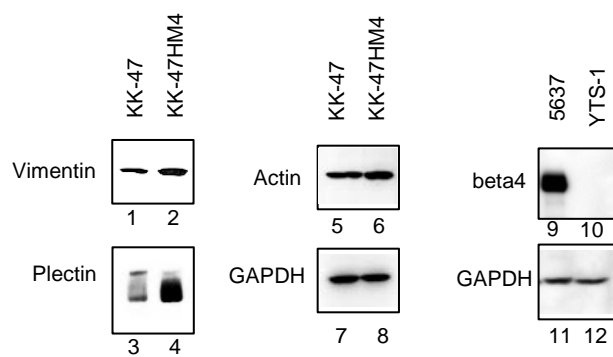


Fig. 4

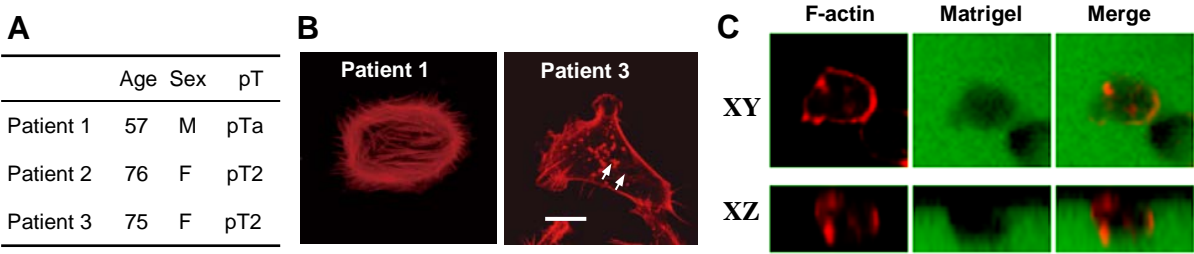


Fig. 5

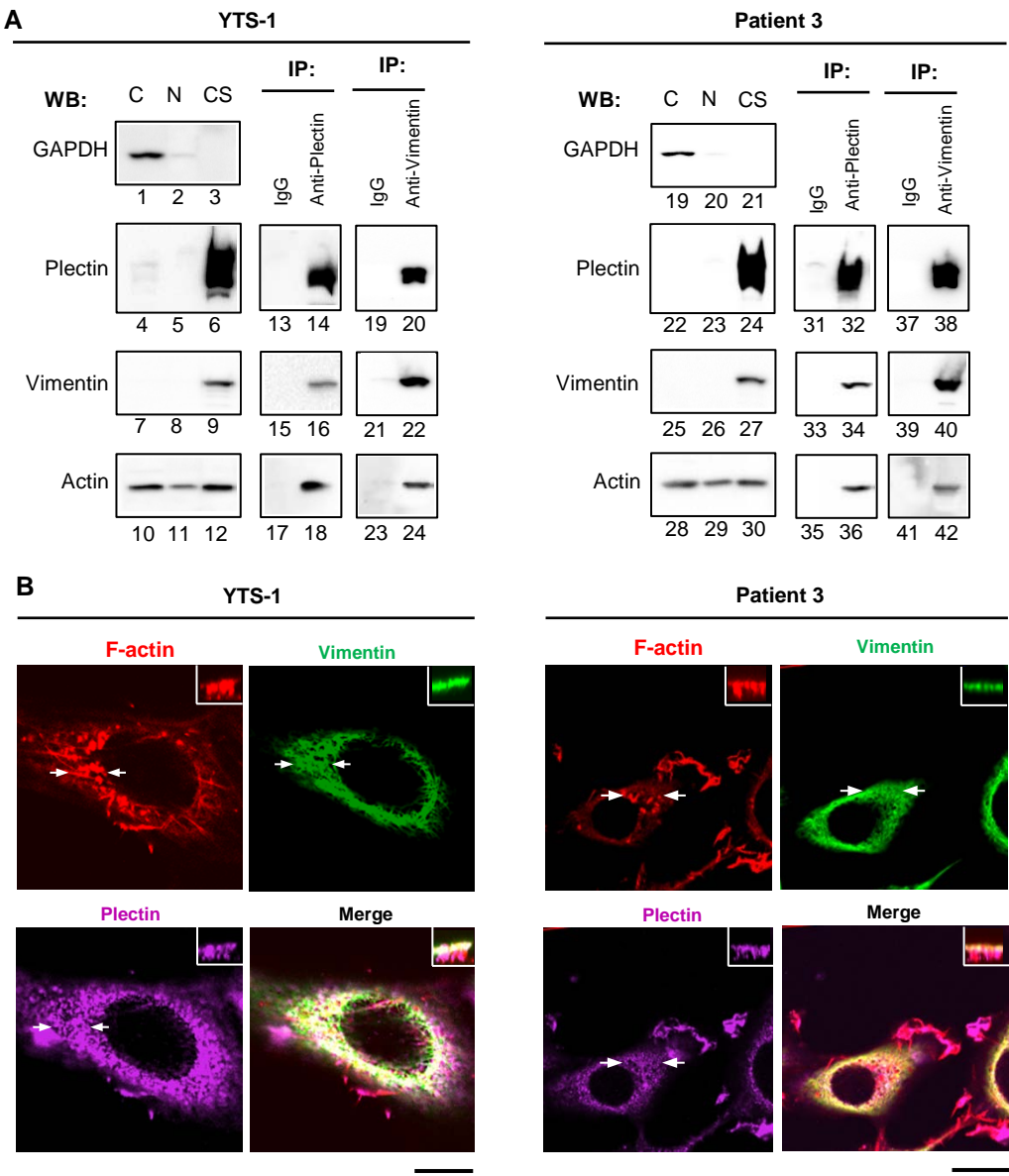


Fig. 6

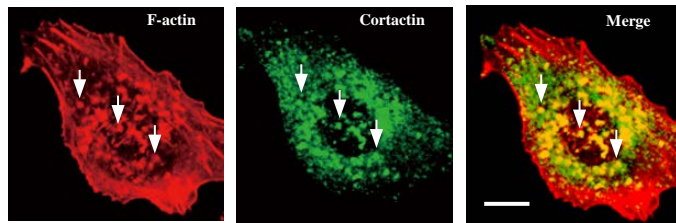


Fig. 7

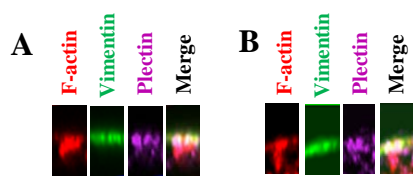


Fig. 8

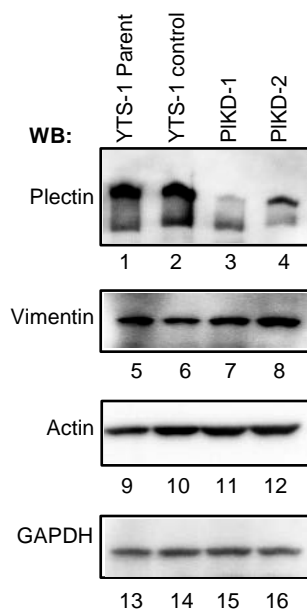


Fig. 9

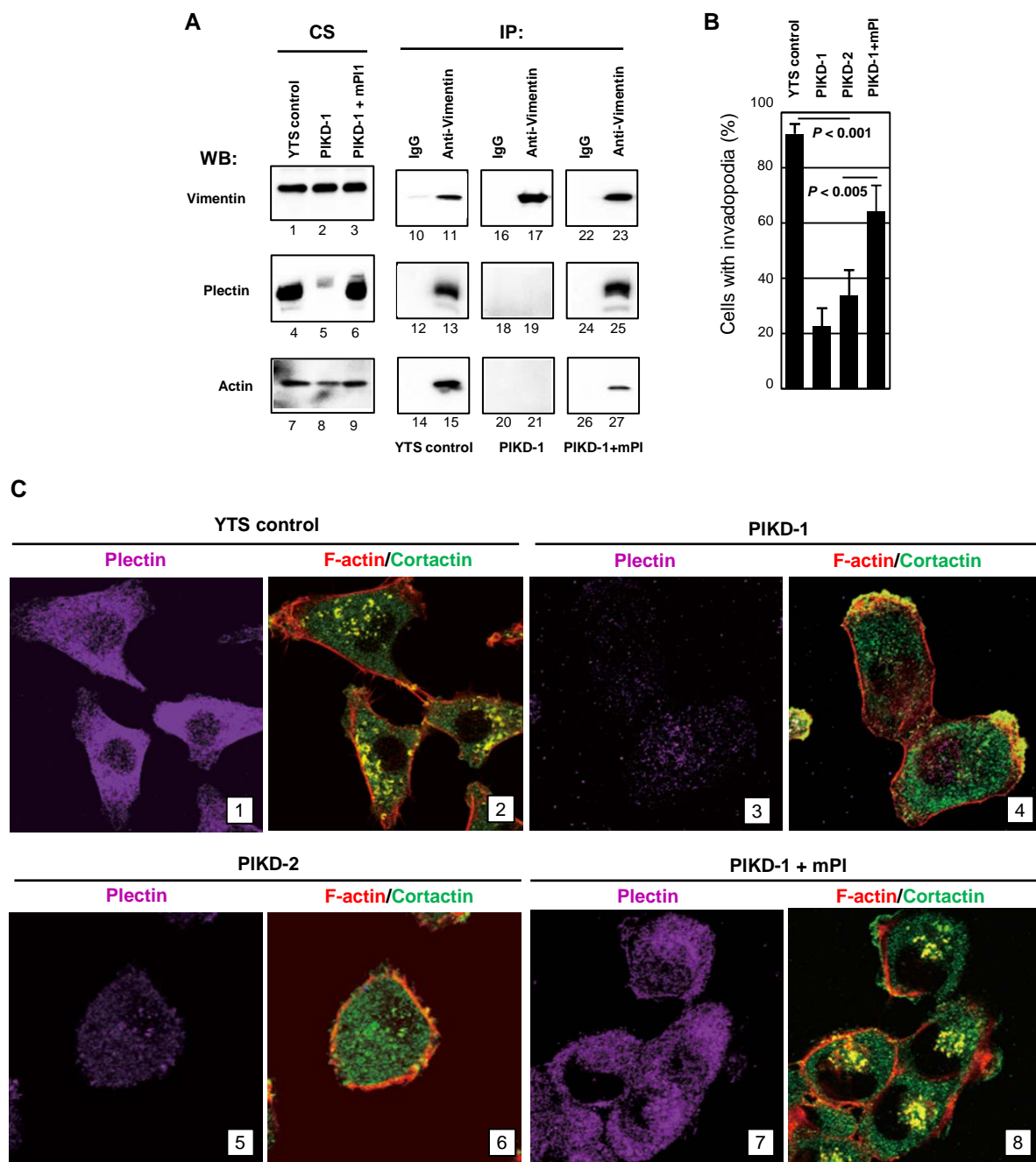


Fig. 10

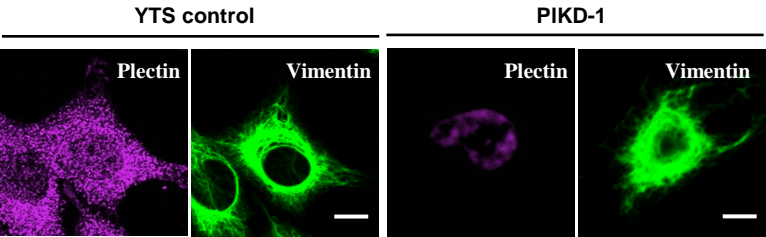


Fig. 11

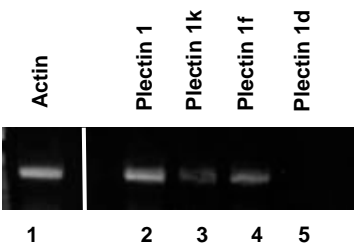


Fig. 12

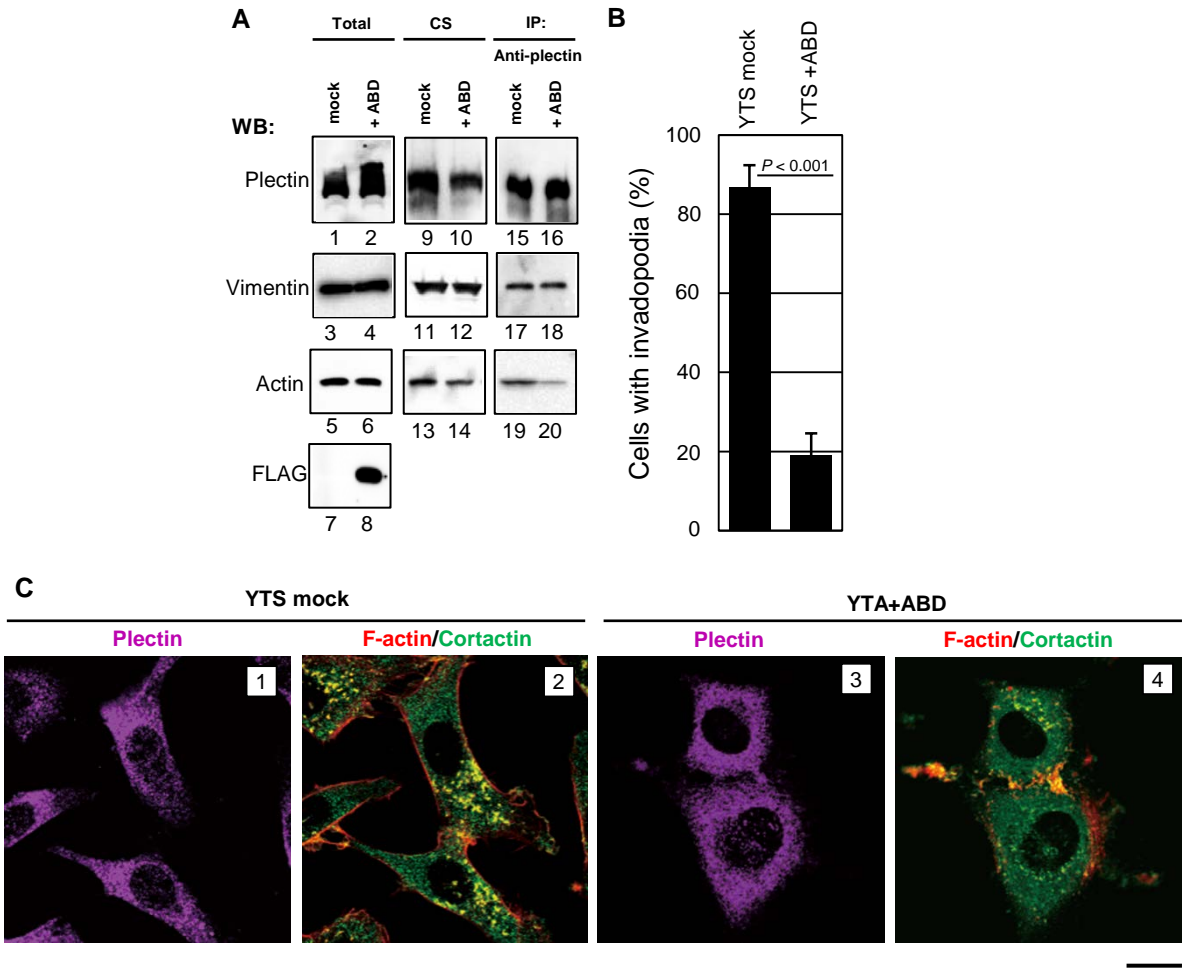


Fig. 13

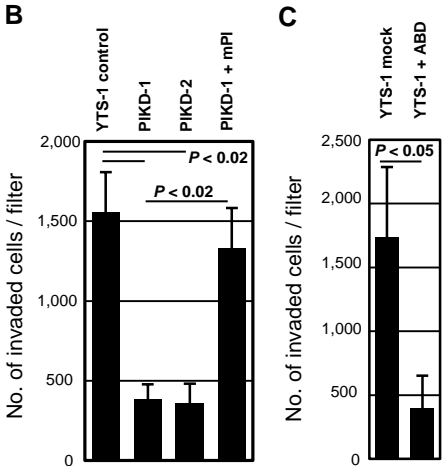
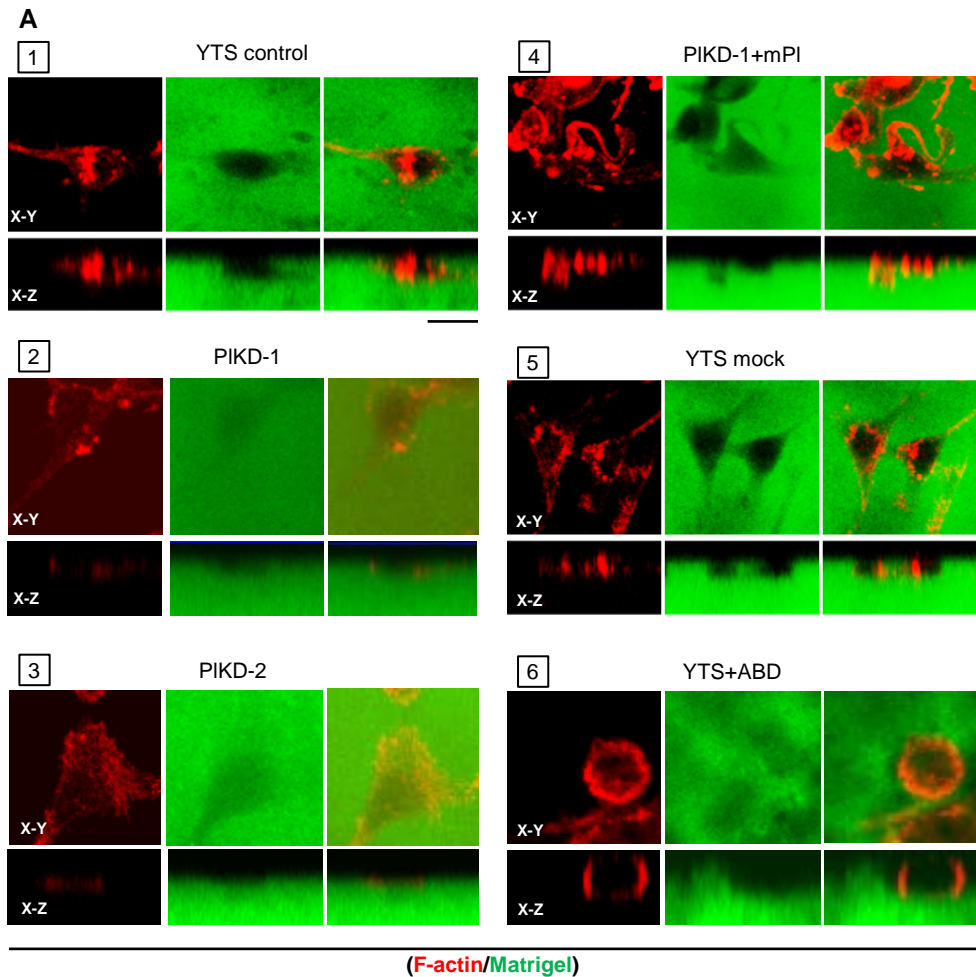


Fig. 14

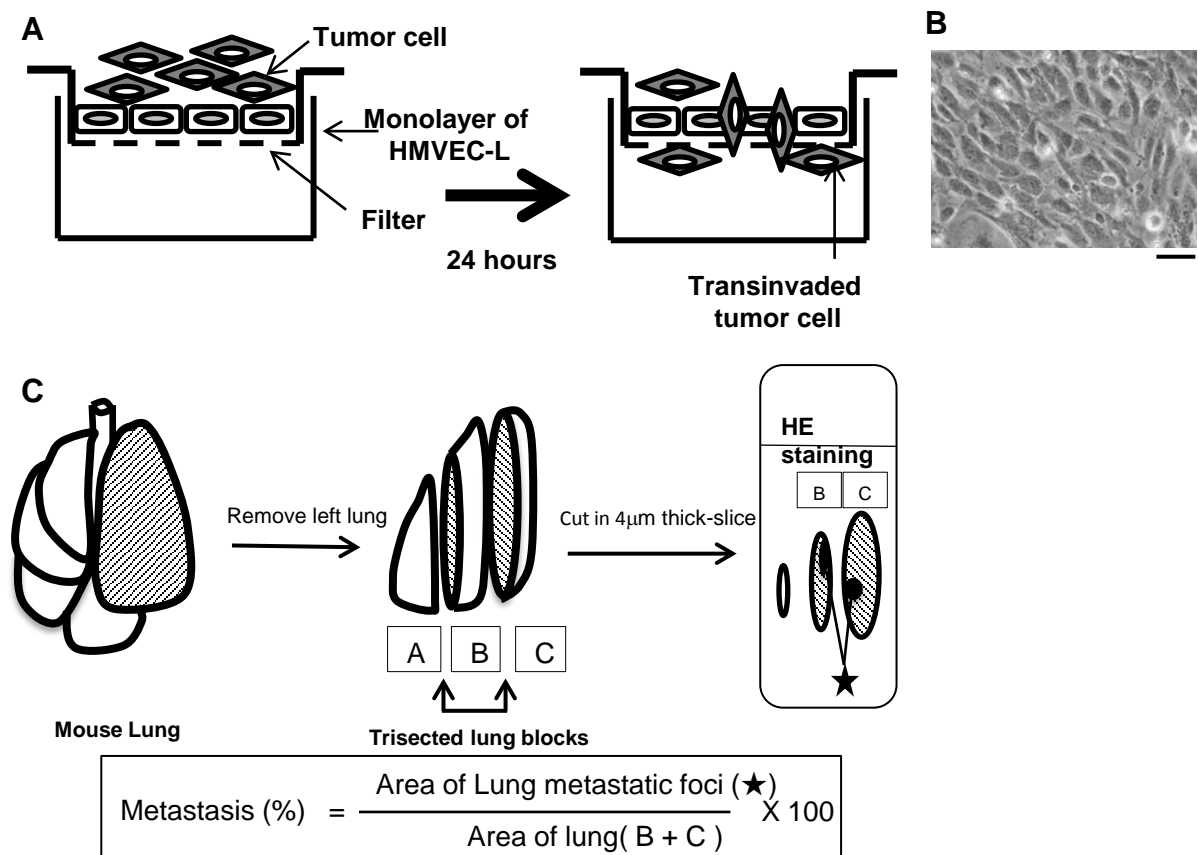


Fig. 15

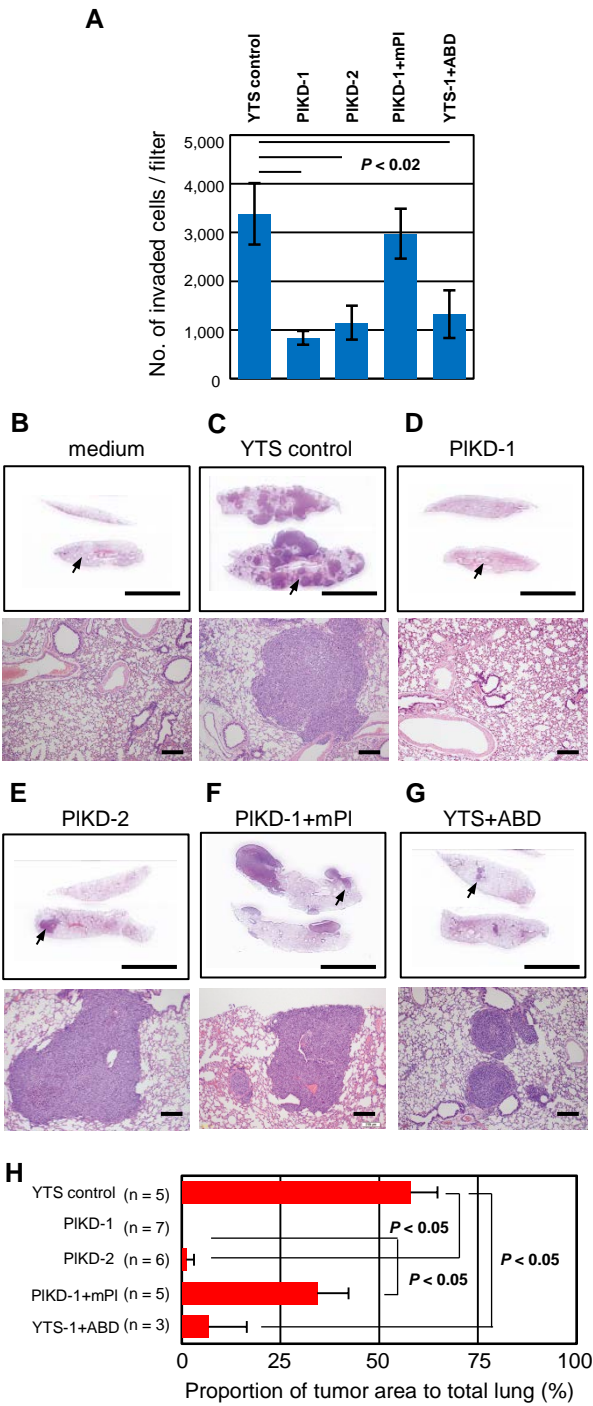


Fig. 16

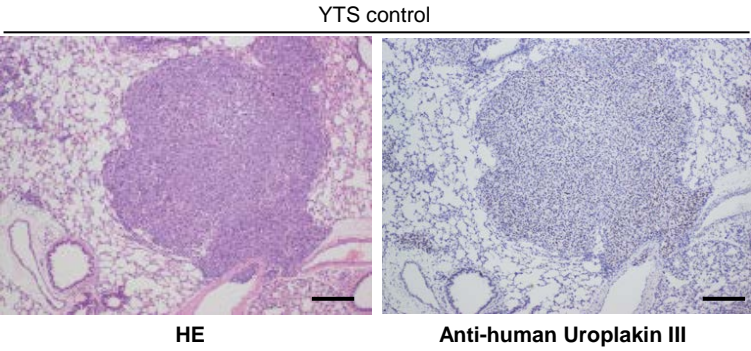


Fig. 17

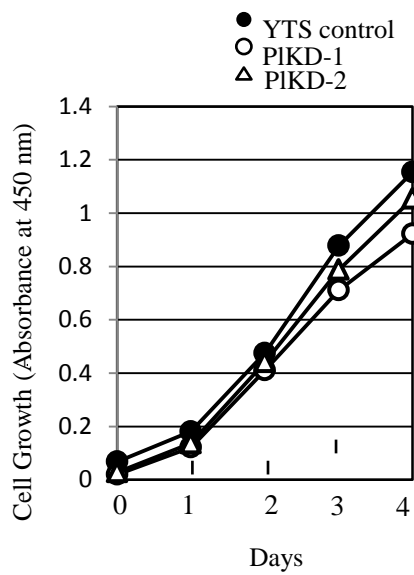


Fig. 18

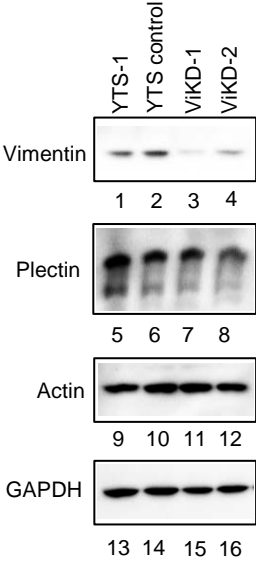


Fig. 19

